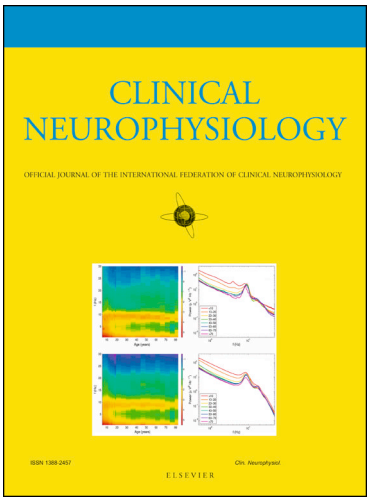

Phase-locked and non-phase-locked EEG responses to pinprick stimulation before and after experimentally-induced secondary hyperalgesia

Emanuel N. van den Broeke, Bart de Vries, Julien Lambert, Diana M. Torta, André Mouraux

PII: S1388-2457(17)30190-6
DOI: http://dx.doi.org/10.1016/j.clinph.2017.05.006
Reference: CLINPH 2008149

To appear in: *Clinical Neurophysiology*

Received Date: 17 December 2016
Revised Date: 8 May 2017
Accepted Date: 12 May 2017

Please cite this article as: van den Broeke, E.N., de Vries, B., Lambert, J., Torta, D.M., Mouraux, A., Phase-locked and non-phase-locked EEG responses to pinprick stimulation before and after experimentally-induced secondary hyperalgesia, *Clinical Neurophysiology* (2017), doi: http://dx.doi.org/10.1016/j.clinph.2017.05.006

Phase-locked and non-phase-locked EEG responses to pinprick stimulation before and after experimentally-induced secondary hyperalgesia

Emanuel N. van den Broeke [1,*], Bart de Vries [1], Julien Lambert [1], Diana M Torta [1,2], André Mouraux [1]

[1] Institute of Neuroscience, Université catholique de Louvain, B-1200, Brussels, Belgium
[2] Faculty of Psychology and Educational Sciences, Health Psychology Group, Katholieke Universiteit Leuven, 3000, Leuven, Belgium

***Corresponding author:**
Emanuel N van den Broeke
Institute of Neuroscience (IoNS)
Faculty of Medicine
Université catholique de Louvain
1200, Brussels
Belgium
E-mail: Emanuel.vandenbroeke@uclouvain.be

Keywords
Central sensitization; pinprick; event-related potentials; brain oscillations; time-frequency

Highlights

- Pinprick stimuli elicit a low-frequency EEG response and a reduction of alpha-band oscillations.
- Secondary hyperalgesia is associated with an increase of the low-frequency EEG response.
- Time-frequency analysis is useful for identifying this increase in low-frequency EEG response.

ABSTRACT

Objective: Pinprick-evoked brain potentials (PEPs) have been proposed as a technique to investigate secondary hyperalgesia and central sensitization in humans. However, the signal-to-noise (SNR) of PEPs is low. Here, using time-frequency analysis, we characterize the

phase-locked and non-phase-locked EEG responses to pinprick stimulation, before and after secondary hyperalgesia.

Methods: Secondary hyperalgesia was induced using high-frequency electrical stimulation (HFS) of the left/ right forearm skin in 16 volunteers. EEG responses to 64 and 96 mN pinprick stimuli were elicited from both arms, before and 20 minutes after HFS.

Results: Pinprick stimulation applied to normal skin elicited a phase-locked low-frequency (<5 Hz) response followed by a reduction of alpha-band oscillations (7-10 Hz). The low-frequency response was significantly increased when pinprick stimuli were delivered to the area of secondary hyperalgesia. There was no change in the reduction of alpha-band oscillations. Whereas the low-frequency response was enhanced for both 64 and 96 mN intensities, PEPs analyzed in the time domain were only significantly enhanced for the 64 mN intensity.

Conclusions: Time-frequency analysis may be more sensitive than conventional time-domain analysis in revealing EEG changes associated to secondary hyperalgesia.

Significance: Time-frequency analysis of PEPs can be used to investigate central sensitization in humans.

1. INTRODUCTION

Intense or sustained nociceptor activation, induced for example by capsaicin or high frequency electrical stimulation (HFS), triggers an activity-dependent long-lasting, but reversible, long-term potentiation (LTP) in spinal nociceptive pathways (Sandkühler, 2007). In humans, topical capsaicin or HFS of the skin induces hyperalgesia in the treated area ("primary" hyperalgesia, LaMotte et al., 1991; Klein et al., 2004; Henrich et al., 2015). This primary hyperalgesia is thought to result from both a peripheral sensitization of nociceptors and LTP in spinal nociceptive pathways (Sandkühler and Gruber-Schoffnegger, 2012).

However, it also results in a pronounced and long-lasting enhancement of mechanical pinprick sensitivity that spreads beyond the treated area ("secondary" hyperalgesia, LaMotte et al., 1991; Klein et al., 2004). The exact mechanism underlying this increased pinprick sensitivity is currently unknown (Sandkühler and Gruber-Schoffnegger, 2012) but several lines of evidence suggest that it results from central sensitization (Baumann et al., 1991; LaMotte et al., 1991; Simone et al., 1991), i.e. an *"increased responsiveness of nociceptive neurons in the central nervous system to their normal or subthreshold afferent input"* (Loeser and Treede, 2008).

To explore the changes in brain activity related to this increased pinprick sensitivity we recently recorded pinprick-evoked brain potentials (PEPs) before and after experimentally induced pinprick hyperesthesia with capsaicin (Van den Broeke et al., 2015). Different pinprick intensities, ranging from 16 to 512 mN, were used to characterize the effect of stimulation intensity on PEPs. We found that when pinprick stimuli were applied inside the area of increased pinprick sensitivity, PEPs elicited by intermediate pinprick intensities were

increased, with the strongest and only significant increase for the 64 mN stimulation intensity. In a follow-up study, we showed that the increase in PEP magnitude followed the long-lasting time course of the increase in pinprick perception (Van den Broeke et al., 2016a). These results suggest that the recording of PEPs could be an interesting tool to evaluate the cortical processing of mechanical nociceptive input in the context of central sensitization, with potential clinical applications.

However, in these previous studies the PEP waveforms were only analyzed in the time-domain. Time-domain averaging assumes that event-related potentials (ERPs) are embedded in background EEG activity that is considered as noise (Dawson, 1954). By averaging signals aligned to the onset of the stimulus, all signals that are not phase-locked to the onset of the stimulus are attenuated, thereby increasing the signal-to-noise ratio (SNR) of phase-locked ERPs. However, variability in the latency of the elicited responses can render ERPs not strictly phase-locked to the stimulus onset. Furthermore, it has been shown that stimuli can also transiently increase or decrease the magnitude of ongoing EEG oscillations, a phenomenon referred to as event-related synchronization and desynchronization (Kalcher and Pfurtscheller, 1995; Mouraux et al., 2003; Ploner et al., 2005; Mouraux and Iannetti, 2008). One way to identify these responses is to estimate the magnitude of EEG oscillations in the time-frequency domain, such as to identify time-locked changes in EEG power regardless of whether the underlying change in signal is phase-locked to the stimulation onset.

In previous studies, the SNR of PEPs identified using conventional time-domain averaging was low, possibly because the stimulus and/or the activity elicited by the activation of mechanoreceptors is not highly phasic, but also because of variability in the force applied

across trials when manually delivering the pinprick stimuli. Using time-frequency analysis of the EEG signals, the aim of the present study was to disclose the phase-locked and non-phase-locked EEG responses to pinprick stimulation and their change when pinprick stimuli are applied to the area of secondary hyperalgesia. We hypothesized that, as compared to PEPs identified in the time domain, this approach might yield pinprick-evoked EEG responses having a higher SNR. In addition, we attempted to further enhance the SNR by improving the reproducibility of pinprick stimulation.

2. MATERIALS AND METHODS

2.1 Participants

Sixteen healthy volunteers took part in the experiment (8 men and 8 women; aged 20 – 27 years; 22.7 ± 2.2 years [mean ± sd]). The experiment was conducted according to the declaration of Helsinki. "Approval for the experiment was obtained from the local Ethical Committee. All participants signed an informed consent form and received financial compensation for their participation (Van den Broeke and Mouraux, 2014b)."

2.2 Experimental design

The design of the experiment is summarized in Figure 1. During the experiment, participants were comfortably seated in a chair with their arms resting on a table in front of them, with palms up. Transcutaneous high frequency electrical stimulation (HFS) of the left or right volar forearm was used to induce increased pinprick sensitivity in the surrounding unconditioned skin (Klein et al., 2004; Van den Broeke and Mouraux, 2014a; 2014b; Van den Broeke et al., 2016a; 2016b). "To avoid any confounding effect of handedness, the arm onto which HFS was applied (dominant vs. non dominant) was counterbalanced across

participants (Van den Broeke and Mouraux, 2014a; 2014b; Van den Broeke et al., 2016a; 2016b)". Handedness was assessed using the Flinders Handedness Survey (Nicolls et al., 2011). Mechanical pinprick stimuli were applied before (pre) and 20 minutes after (post) applying HFS. The stimuli were delivered to the skin surrounding the area onto which HFS was delivered, and to the corresponding skin area of the contralateral arm that served as control. During the pinprick stimulation, a vertical white curtain (46 x 42 cm) was placed over both arms at the level of the cubital fossa to prevent view of the arms. Two experimenters were sitting at the opposite side of the table; one performing the pinprick stimulation and one collecting the behavioral scores.

2.3 Induction of increased pinprick sensitivity

HFS was applied to the volar forearm, 10 cm distal to the cubital fossa and consisted of five trains of 100 Hz electrical pulses (pulse width: 2 ms) lasting 1 s each. The time interval between each train was 10 s. The intensity of stimulation was individually adjusted to 20x the absolute detection threshold to a single pulse (0.29 ± 0.09 mA; mean ± sd). The electrical pulses were triggered by a programmable pulse generator (Master-8; AMPI Israel), produced by a constant current electrical stimulator (Digitimer DS7A, Digitimer UK), and delivered to the skin using a specifically designed electrode designed and built at the Centre for Sensory-Motor Interaction (Aalborg University, Denmark, see also Van den Broeke and Mouraux, 2014a; 2014b; Van den Broeke et al., 2016a; 2016b). The cathode consists of 16 blunt stainless steel pins with a diameter of 0.2 mm protruding 1 mm from the base. The 16 pins are placed in a circle with a diameter of 10 mm. The anode consists of a surrounding stainless steel ring having an inner diameter of 22 mm and an outer diameter of 40 mm.

2.4 Mechanical pinprick stimulation

A custom-built calibrated handheld pinprick stimulator was used to deliver the mechanical pinprick stimuli (Van den Broeke et al., 2016a). The stimulator consists of a cylindrical stainless steel flat tip probe (diameter: 0.35 mm, uniform geometry) on top of which rests a calibrated cylindrical weight. The probe and weight are mounted inside an aluminum tube. When applied perpendicular to the skin, the probe and weight slide freely inside the tube. Once the probe is maintained against the skin, it generates a constant normal force entirely determined by the mass of the probe and weight.

Two intensities of pinprick stimulation were used (64 and 96 mN). For each intensity of pinprick stimulation, each arm (HFS and control arm) and each time point (pre and post), a total of thirty stimuli were administered. "The pinprick stimuli were delivered by applying the probe, from a distance of approximately 5 mm above the skin, slowly onto the skin and moving the tube downwards and upwards with a total duration of approximately one second (Van den Broeke et al., 2015; see also video 1)". The exact timing of stimulation was provided through headphones to the experimenter that performed the pinprick stimulation. Each trial consisted of a preparation tone (80 ms) followed after 1 sec. by a 1 second tone during which the pinprick stimulation was delivered. Each stimulus was delivered 8 seconds after the moment the participant reported the quality of sensation and/or rating of the preceding stimulus. The pinprick stimulation was always performed by the same experimenter. We hypothesized that an optimal control of the applied forces onto the skin may improve the reproducibility of the EEG responses and, thereby, increase the signal-to-noise ratio of PEPs. Therefore, before conducting the experiment, the experimenter who performed the pinprick stimulation underwent a training in which he practiced to deliver

stable and reproducible forces during pinprick stimulation, using a 6-axis strain-gauge force-torque transducer (Nano 43, ATI Industrial Automation, Inc., Apex, NC, USA) to provide on-line feedback of the applied normal and tangential forces. Before training considerable variability in the applied normal and tangential forces were observed (Supplementary Figure S1). After training the forces generated by the pinprick stimulation were markedly more stable.

The order of presentation of the two pinprick intensities, as well as the arm onto which stimuli were first applied (HFS vs. control arm) were counterbalanced across participants. "To avoid sensitization of the stimulated skin, the target of the pinprick stimulus was displaced after each stimulus (Van den Broeke et al., 2015)".

2.5 Intensity and quality of perception

Participants were asked to indicate directly after each pinprick stimulus whether the stimulus was perceived as pinprick, touch or undetected. Participants were familiarized with both sensations (touch and pinprick) at the beginning of the experiment by applying gently the two sides of a pushpin onto the skin. Moreover, within each block of thirty stimuli, participants were asked to rate the intensity of the percept elicited by ten randomly selected stimuli using a numerical rating scale (NRS) ranging from 0 (no perception) to 100 (maximal pain), with 50 representing the transition from non-painful to painful domains of sensation (Van den Broeke and Mouraux, 2014a; 2014b; Van den Broeke et al., 2016a). To assess changes in intensity of perception we performed, for both stimulation intensities (64 and 96 mN), a General Linear Model (GLM) repeated measures ANOVA analysis using two within-subject factors: time (pre vs. post) and treatment (control vs. HFS arm). The dependent

variable was the NRS score (average of the 10 ratings). The level of significance was set at $p<0.05$. For post-hoc tests, *p*-values were Bonferroni corrected for the number of tests. In our case the *p*-value was divided by two ($p<0.025$) as we compared the effect of time separately for each arm (control and HFS). The statistical analyses were conducted using SPSS 18 (SPSS Inc., Chicago, IL, USA). The effect of HFS was assessed using the interaction between the factors time and treatment.

2.6 EEG recording

"The EEG was recorded using 32 actively shielded Ag-AgCl electrodes that were mounted in an elastic cap and arranged according to the international 10-20 system (Waveguard32 cap, Advanced Neuro Technologies, The Netherlands, Van den Broeke and Mouraux, 2014a)". Participants were instructed to sit as still as possible and keep their gaze fixed on a black cross displayed at a distance of approximately 2 m. "The EEG signals were amplified and digitized using a sampling rate of 1000 Hz and an average reference (HS32; Advanced Neuro Technologies, The Netherlands). Eye movements were recorded using two surface electrodes placed at the upper-left and lower-right sides of the left eye (Van den Broeke and Mouraux, 2014a)". Electrode impedances were kept below 20 kΩ. To generate a trigger in the EEG that marked the actual time at which the probe touched the skin, we used a high resistance switch triggered by the change in impedance occurring between the probe and a ground electrode placed against the skin at the wrist. A thin layer of conductive gel was used to lower the impedance between the probe and the skin. The delay between the contact of the skin and the generation of the trigger was almost zero (0.046 ± 0.015 ms; Van den Broeke et al., 2016a).

2.7 EEG analysis

The EEG signals were analyzed offline using Letswave 6.0 (www.nocions.org/letswave).

2.7.1 Time-domain analysis

After applying a 0.3- 30 Hz band pass zero-phase Butterworth filter to the continuous EEG recordings, the signals were segmented into epochs extending from -500 to +1500 ms relative to stimulus onset. Epochs contaminated by eye movements or eye blinks were corrected using an Independent Component Analysis (ICA; (Jung et al., 2000)). Denoised epochs were then baseline-corrected (reference interval: -500 to 0 ms) and re-referenced to linked earlobes (A1A2). Finally, epochs with amplitude values exceeding ±100 µV were rejected as these were likely to be contaminated by artifacts.

Separate averaged waveforms were computed for each participant, time point (pre and post), stimulation site (HFS and control) and stimulation intensity (64 and 96 mN). To assess whether there was a significant difference after HFS between PEPs elicited from both stimulation sites, we used a non-parametric cluster-based permutation approach (Groppe et al., 2011; Maris and Oostenveld, 2007, but see also Van den Broeke et al., 2015; 2016a). The advantages of this approach are that it does not rely on the subjective visual identification of peaks in the PEP waveforms and that it provides a simple way to solve the problem of multiple comparisons (Maris and Oostenveld, 2007). As a first step, we computed, for each subject and electrode, difference waveforms assessing the change in PEP waveform at post vs. pre at the control arm (control arm_{post} – control arm_{pre}) and at the HFS-treated arm (HFS arm_{post} – HFS arm_{pre}). Then, we performed the cluster-based permutation test on the difference waveforms of both arms, thereby testing the time x treatment interaction. Based

on the results of our previous studies (Van den Broeke et al., 2015; 2016a) we performed the permutation test only on the midline central-posterior electrodes (Cz and Pz). The test consisted of the following steps (adapted from Van den Broeke et al., 2015; 2016a and summarized here). "First, the difference waveforms were compared by means of a point-by-point paired-sample t-test. Then, samples above the critical t-value for a parametric two-sided test that were adjacent in time were identified and clustered. An estimate of the magnitude of each cluster was then obtained by computing the sum of the absolute t-values constituting each cluster (cluster-level statistic). Random permutation testing (2000 times) of the subject-specific difference waveform of the two arms (performed independently for every subject) was then used to obtain a reference distribution of maximum cluster magnitude. Finally, the proportion of random partitions that resulted in a larger cluster-level statistic than the observed one (i.e. p-value) was calculated. Clusters in the observed data were regarded as significant if they had a magnitude exceeding the threshold of the 97.5th percentile of the permutation distribution." This corresponds to a critical alpha-level of 0.05 when the test is performed at two electrodes (Cz and Pz).

2.7.2 Time-frequency analysis of low-frequency activities (1-30 Hz)

A short-time fast Fourier transform (STFFT) with a fixed Hanning window of 500 ms was used to decompose the band-pass filtered (0.3-30 Hz) and ICA-denoised EEG signals used for the time-domain analysis. The explored frequencies ranged from 1 to 30 Hz. To identify pinprick-evoked EEG activity that is not necessarily phase-locked to the onset of the pinprick stimulus, the STFFT was applied to each single EEG epoch (TF-SINGLE). Then, the single-trial time-frequency estimates of oscillation amplitude were averaged across trials, separately for each subject and condition. To distinguish phase-locked and non-phase-locked EEG

responses in the time-frequency domain, the STFFT was also applied to the averaged waveforms obtained after time-domain averaging (TF-AVERAGE). Furthermore, we calculated the phase-locking value (PLV) using the single-trial time-frequency estimates of phase (Mouraux and Iannetti, 2008). To assess the effect of HFS on the EEG responses identified in the time-frequency domain, we used the same non-parametric cluster-based permutation approach that was used to analyze signals in the time domain, but applied to the TF-SINGLE time-frequency maps obtained at electrodes Cz and Pz. First, we computed for each subject difference time-frequency maps assessing the change in amplitude at post vs. pre at the control arm (control arm_{post} – control arm_{pre}) and at the HFS-treated arm (HFS arm_{post} – HFS arm_{pre}). Then, we applied the cluster-based permutation test on the difference maps of both arms, thereby testing the time x treatment interaction. Importantly, the cluster-based permutation test was adapted to cluster adjacent time *and* frequency points. "Clusters in the observed data were regarded as significant if they had a magnitude exceeding the threshold of the 97.5^{th} percentile of the permutation distribution". This corresponds to a critical alpha-level of 0.05 when the test is performed at two electrodes. Finally, to visualize changes in post-stimulus EEG activity relative to the pre-stimulus baseline period, a baseline correction was applied. For this, the average amplitude of the EEG signal between -500 and -100 ms relative to stimulus onset was subtracted from each post-stimulus time point. This was performed separately for each estimated frequency (Hu et al., 2014).

2.7.3 Time-frequency analysis of high-frequency activities (30-100 Hz)

To examine whether pinprick stimulation also elicited changes in the magnitude of high-frequency activities (>30 Hz), the continuous EEG signals were band-pass filtered using a 30-

100 Hz band pass zero-phase Butterworth filter and a notch filter between 49 and 51 Hz. After segmenting the signals from -500 to +1500 ms relative to stimulation onset, and ICA-denoising, single-trial time-frequency estimates of signal amplitude and phase were generated using as short-time fast Fourier transform (STFFT) with a fixed Hanning window of 200 ms. The explored frequencies ranged from 30 to 100 Hz. The obtained time-frequency estimates were analyzed using the same approach used for the analysis of low-frequency activities. To visualize changes in post-stimulus EEG activity relative to the pre-stimulus baseline period, the same baseline correction method as for the low-frequency activities was applied but between -500 and 0 ms relative to stimulus onset. A common issue of high-frequency activities recorded using scalp EEG electrodes is that these activities are not necessarily of electro-cortical origin but instead, can reflect muscular activity and/or eye-movement related activity (Muthukumaraswamy, 2013). For this reason, the same analyses (but without ICA) were performed using the bipolar EOG recordings obtained from the two surface electrodes placed at the upper-left and lower-right sides of the left eye.

3. RESULTS

3.1 Intensity of perception

HFS induced a clear increase in pinprick sensitivity at the HFS arm, as shown by the changes in the intensity of the percept elicited by both 64 mN and 96 mN pinprick stimulation (Figure 2A). This was confirmed by the repeated-measures ANOVA, which showed a significant time × treatment interaction for both the 64 mN stimulus ($F(1, 15) = 61.279$, $p < .001$, partial $\eta^2 = .803$) and the 96 mN stimulus ($F(1, 15) = 60.428$, $p < .001$, partial $\eta^2 = .801$). Post-hoc tests showed, for both intensities, a statistically significant increase of the perceived intensity at

the HFS-treated arm after HFS (64 mN: paired t-test; t (15) = -6.827, p < .001; 90 mN: t (15) = -8.172, p < .001). No significant changes in perceived intensity were observed at the control arm.

3.2 Quality of perception

Before applying HFS, both the 64 mN and the 96 mN pinprick stimuli were qualified as 'pinprick' in approximately 75% of the trials, and as 'touch' in the remaining 25% of the trials (Figure 2B). This was also the case for the pinprick stimuli delivered to the control arm after HFS. In contrast, almost all pinprick stimuli delivered to the treated arm after HFS were qualified as 'pinprick'.

3.3. Time-domain analysis of PEPs

Both the 64 mN and the 96 mN pinprick stimuli elicited a clear positive wave peaking approximately 350 ms after stimulus onset (Figure 3 and 4). As compared to the PEP waveforms obtained in our previous studies (Van den Broeke et al., 2015; 2016a), the signal-to-noise ratio of this response was clearly increased (Supplementary Figure S2).

3.3.1 PEPs elicited by the 64 mN pinprick stimulus

The group-level average waveforms of the PEPs elicited by the 64 mN stimulation are shown in Figure 3A. The results of the cluster-based permutation test performed on the PEP difference waveforms (post vs. pre HFS) of both arms (control vs. HFS) revealed a cluster having a p-value smaller than the critical alpha level of 0.025 at both electrode Cz (Fig. 3B) and Pz. The cluster at Cz extended between 290 and 460 ms (p=0.0046). The cluster at Pz

extended between 320 and 470 (p=0.0013). To assess whether the difference in PEP amplitude after HFS was due to an increase of PEP amplitude at the HFS-treated arm, a decrease of PEP amplitude at the control arm, or both, we performed post-hoc tests (paired t-tests, two-sided, Bonferroni corrected) on the individual mean amplitude values calculated within the cluster. The paired t-tests revealed a significant increase in mean PEP amplitude after HFS compared to before HFS at the HFS arm, both at electrode Cz (t (15) =-3.375, p=0.004, Figure 3C), and at electrode Pz (t (15) =-4.486, p<.001). No significant changes in mean PEP amplitude were observed for the control arm. The increase in PEP amplitude was maximal at central-posterior scalp electrodes (Fig. 3D).

3.3.2 PEPs elicited by the 96 mN pinprick stimulus

The group-level average waveforms of the PEPs elicited by 96 mN stimulation are shown in Figure 4. The permutation test did not identify any cluster having a p-value smaller than the critical alpha level of 0.025.

3.4 Time-frequency analysis of low-frequency activities (1-30 Hz)

3.4.1 EEG responses elicited by the 64 mN pinprick stimulus

The group-level average TF-SINGLE time-frequency map of EEG amplitude measured at electrodes Cz is shown in Figure 5A. This map shows that the pinprick stimulus elicited (1) a marked increase of low-frequency activities (<5 Hz) extending between 150-400 ms in the time domain and (2) a long-lasting decrease of alpha-band oscillations extending between 300-600 ms in the time domain and 7-10 Hz in the frequency domain. The same increase of low-frequency activities was observed in the TF-AVERAGE time-frequency map (Figure 5B), indicating that this response corresponded to the time-frequency representation of the PEP

identified in the time domain. This was also confirmed by the PLV time-frequency map, (Figure 5C) showing that, at these latencies and frequencies, the EEG signals were markedly phase-locked to the stimulation onset. The group-level average time-frequency maps obtained at both time points (pre and post HFS) and arms (control and HFS) are shown in Figure 6A. The results of the cluster-based permutation test performed on the *difference* TF-SINGLE time-frequency maps (post vs. pre HFS) of both arms (control vs. HFS) revealed a positive cluster having a p-value smaller than the critical alpha level of 0.025 both at electrode Cz ($p=0.0052$; Fig. 6B), and at electrode Pz ($p=0.0242$). This cluster clearly circumscribed the phase-locked low-frequency response corresponding to the PEP identified in the time-domain. To assess whether the difference in magnitude of the low frequency response after HFS was due to an increase at the HFS-treated arm, a decrease at the control arm, or both, we performed post-hoc tests (paired t-tests, two-sided, Bonferroni corrected) on the individual mean amplitude values calculated within the cluster, at electrode Cz. The paired t-tests revealed a significant increase in mean amplitude after HFS compared to before HFS at the HFS arm ($t(15) = -6.217$, $p<0.001$, Figure 6C). No significant changes in mean amplitude were observed for the control arm.

3.4.2. EEG responses elicited by the 96 mN pinprick stimulus

The group-level average time-frequency maps obtained at both time points (pre and post HFS) and arms (control and HFS) are shown in Figure 7A. Such as for the 64 mN stimulus, the cluster-based permutation test revealed a positive cluster having a p-value smaller than the critical alpha level of 0.025 at electrode Cz ($p=0.0090$; Fig. 7B). Again, this cluster clearly circumscribed the phase-locked low-frequency response corresponding to the PEP identified in the time-domain. No cluster with a p-value smaller than the critical alpha level of 0.025

was identified at electrode Pz. To assess whether the difference in low frequency response after HFS was due to an increase at the HFS-treated arm, a decrease at the control arm, or both, we performed post-hoc tests on the individual mean amplitude values calculated within the cluster, at electrode Cz. The paired t-tests revealed a significant increase in mean amplitude after HFS compared to before HFS at the HFS arm (t (15) =-3.310, p=0.005, Figure 7C). No significant changes in mean amplitude were observed for the control arm.

3.5 Time-frequency analysis of high-frequency activities (30-100 Hz)

3.5.1 High frequency activity elicited by the 64 mN pinprick stimulus

The group-level average time-frequency maps of high-frequency activities are shown in Figure 8. The permutation testing did not reveal any cluster having a p-value smaller than the critical alpha level of 0.025.

3.5.2 High frequency activity elicited by the 96 mN pinprick stimulus

The group-level average time-frequency maps of high-frequency activities are shown in Figure 9A. The permutation testing revealed two clusters having a p-value smaller than the critical alpha level of 0.025 for electrode Cz (Fig. 9B). The first cluster extended between 600-1000 ms and 40-90 Hz (p=0.017), the second cluster between 1000-1500 ms and 30-100 Hz (p=0.0061). For electrode Pz, the permutation test revealed a cluster between 800-1500 ms and 30-100 Hz (p=0.0077).

Crucially, the same increase of high-frequency activities was observed in the bipolar recordings of the EOG signals (Supplementary Figure S3). In fact, the increase in high-frequency activities was clearly more prominent in the signals recorded by these

extracephalic electrodes as compared to the signals recorded from the scalp, indicating that these activities most probably corresponded to electromyographic activity triggered by the pinprick stimulation.

3.6 Effect size comparison between time-frequency and time domain analysis

The effect size of the increase in amplitude of low frequency EEG activities identified in the time-frequency domain at electrode Cz for the 64 mN stimulus (partial η^2 = .685) was larger than the effect size of the increase in PEP amplitude identified in the time domain (partial η^2 = .572).

4. DISCUSSION

The present study confirms that pinprick stimulation applied to the area of secondary hyperalgesia elicits a significantly increased PEP that is most prominent when an intermediate stimulation intensity is used (64 mN), and not so readily identifiable when a stronger stimulation intensity is used (96 mN). Such as in our previous studies (Van den Broeke et al., 2015; 2016a), this enhancement involved a positive wave extending 300-400 ms after stimulation onset, and maximal at central-posterior electrodes. A similar enhancement was observed when analyzing the EEG signals in the time-frequency domain. This enhancement circumscribed a low frequency (<5 Hz) EEG response extending 150-400 ms after stimulus onset. This low-frequency response was largely phase-locked to the onset of stimulation, indicating that it predominantly corresponded to the time-frequency

representation of the PEP identified in the time domain. Interestingly, a significant enhancement of this response was observed for both the 64 mN stimulation and the 96 mN stimulation, suggesting that time-frequency analysis may be more sensitive than conventional time-domain analysis for detecting HFS-induced differences in pinprick-evoked EEG responses. Time-frequency analysis of the EEG signals also showed that the pinprick stimulus induced a reduction of the magnitude of alpha-band oscillations (7-10 Hz). However, this response was largely unaffected by HFS. Finally, time-frequency analysis of high-frequency EEG oscillations showed a clear increase in the magnitude of high frequency (30-100 Hz) activities. However, this increase of high-frequency activities was most pronounced in the electro-oculogram, indicating that these high-frequency signals did not originate from brain activity and instead, most probably resulted from changes in muscle activity.

4.1 The increase in PEP magnitude is maximal for intermediate intensities of pinprick stimulation

The results of the present study confirm those of our previous studies (van den Broeke et al., 2015; 2016a) showing that the increase of PEP magnitude associated with secondary hyperalgesia is more prominent for stimuli of intermediate intensity (64 mN) as compared to stimuli of higher intensity (96 mN). The latency at which the increase in PEP was observed in the present study (290-470 ms) was similar to that of our previous study (van den Broeke et al., 2015), and is compatible with the conduction velocity of A-fiber nociceptors. It remains unclear why the enhancement of PEPs is maximal at intermediate intensities of stimulation (64 mN), whereas a similar increase in pinprick perception is observed at both intermediate

and high intensities of stimulation (64 and 96 mN). In our previous study using capsaicin to induce increased pinprick sensitivity, we found a non-linear inverted U-shape relationship between pinprick stimulation intensity and PEP enhancement. One possibility, although speculative, could be that of a ceiling effect: at high intensities of stimulation, the PEP elicited at baseline may have already reached a maximum, and is thus not further enhanced after HFS (Van den Broeke et al., 2015).

4.2 Time-frequency analysis of PEPs

Time-frequency analysis of the EEG signals showed that, in addition to eliciting a phase-locked PEP, mechanical pinprick stimulation also induced a long-lasting decrease of the magnitude of alpha-band EEG oscillations (7-10 Hz), a phenomenon that is also observed for other sensory stimuli, including nociceptive laser stimulation (Mouraux et al., 2003; Ploner et al., 2005). However, this alpha-band desynchronization did not appear to be affected by HFS. In contrast, a marked increase of the power within high frequency bands (30-100 Hz) was observed after HFS. However, this increase of power at high-frequencies was most prominent in the electro-oculographic signals recorded from the bipolar electrodes located around the eyes, indicating that this activity predominantly reflected muscular activity (Supplementary Figure S2). Finally, although some previous studies suggested that nociceptive laser stimuli may elicit an early-latency enhancement of high-frequency activities within the range of gamma oscillations, maximal at contralateral central electrodes (Gross et al., 2007; Zhang et al., 2012; Hu et al., 2014; Tu et al., 2016), no such enhancement was observed in the present study.

Although the time-frequency analysis did not identify non-phase-locked EEG responses that were modulated by HFS, it did appear to be more sensitive at identifying the HFS-induced change of magnitude of the phase-locked low-frequency PEP. Indeed, a significant enhancement of the time-frequency representation of this component was observed not only for the 64 mN stimulus, but also for the 96 mN stimulus. This could be explained by the fact that estimates of response magnitude obtained in the time-frequency domain are not strongly affected by temporal jitter (Mouraux and Iannetti, 2008). In contrast, across-trial jitter in response latencies is known to have a strong effect on the magnitude of ERP waveforms obtained after across-trial averaging in the time domain (Mouraux and Iannetti, 2008).

4.3 Improving the reproducibility of mechanical pinprick stimulation enhances the SNR of pinprick-evoked brain potentials

In our previous studies (van den Broeke et al., 2015; 2016a), the signal-to-noise ratio of PEPs was low, possibly because of the large variability in applied forces across stimulus repetitions. In the present study, we improved the reproducibility of the applied mechanical pinprick stimuli, and found that this enhances the SNR of PEPs. This has important implications for the potential clinical use of PEPs. First, because the possibility to record these responses with a higher SNR opens the possibility to interpret these responses at individual level. Second, because it shows the importance of applying the stimuli in an operator-independent fashion, for example, by developing a robotic system to deliver the stimuli.

4.4 Clinical usefulness of pinprick-evoked EEG responses

Secondary hyperalgesia, manifested as increased pinprick sensitivity, is thought to be the result of central sensitization (Baumann et al., 1991; LaMotte et al., 1991; Simone et al., 1991). Neuropathic pain is often accompanied by mechanical hyperalgesia (Jensen and Finnerup, 2014; Maier et al., 2010) that is very similar to secondary hyperalgesia. The recording of pinprick-evoked EEG responses could constitute a way to reliably assess the functional status of mechanical nociceptive pathways and to provide a less subjective measure for central sensitization.

4.5 Conclusion

The present study shows that the detection of the enhanced EEG responses to mechanical pinprick stimuli associated with secondary hyperalgesia can be improved (1) by assessing the magnitude of pinprick-evoked EEG responses in the time-frequency domain and (2) by optimizing the reproducibility of pinprick stimulation.

CONFLICT OF INTEREST

None of the authors have potential conflicts of interest to be disclosed.

ACKNOWLEDGEMENTS

EvdB, JL and AM are supported by the ERC “Starting Grant” (PROBING PAIN 336130). BdV is supported by the Erasmus+ programme of the European Commission. DT is supported by the ‘‘Asthenes’’ long-term structural funding Methusalem grant (# METH/15/011) by the Flemish Government, Belgium.

REFERENCES

Baumann TK, Simone DA, Shain CN, LaMotte RH. Neurogenic hyperalgesia: the search for the primary cutaneous afferent fibers that contribute to capsaicin-induced pain and hyperalgesia. J Neurophysiol 1991; 66: 212–227.

Dawson GD. A summation technique for the detection of small evoked potentials. Electroencephalogr Clin Neurophysiol 1954; 6 (1): 65-84.

Gross J, Schnitzler A, Timmermann L, Ploner M. Gamma oscillations in human primary somatosensory cortex reflect pain perception. Plos Biol 2007; 5 (5): e133.

Groppe DM, Urbach TP and Kutas M. Mass univariate analysis of event-related brain potentials/fields I: a critical tutorial review. Psychophysiology 2011; 48: 1711–1725.

Henrich F, Magerl W, Klein T, Greffrath W, Treede RD. Capsaicin-sensitive C- and A-fibre nociceptors control long-term potentiation-like pain amplification in humans. Brain 2015; 138 (9): 2505-20.

Hu L, Xiao P, Zhang ZG, Mouraux A, Iannetti GD. Single-trial time-frequency analysis of electrocortical signals: baseline correction and beyond. Neuroimage 2014; 84: 876-87.

Jensen TS, Finnerup NB. Allodynia and hyperalgesia in neuropathic pain: clinical manifestations and mechanisms. Lancet Neurol 2014; 13(9): 924-35.

Jung TP, Makeig S, Humphries C, Lee TW, McKeown MJ, Iragui V, et al. Removing electroencephalographic artifacts by blind source separation. Psychophysiology 2000; 37: 163–178.

Kalcher J, Pfurtscheller G. Discrimination between phase-locked and non-phase-locked event-related EEG activity. Electroencephalogr Clin Neurophysiol 1995; 94(5): 381-4.

Klein T, Magerl W, Hopf HC, Sandkühler J, Treede RD. Perceptual correlates of nociceptive long-term potentiation and long-term depression in humans. J Neurosci 2004; 24 (4): 964-71.

LaMotte RH, Shain CN, Simone DA and Tsai E-F. Neurogenic hyperalgesia: psychophysical studies of underlying mechanisms. J Neurophysiol 1991; 66: 190–211.

Loeser JD, Treede R. The Kyoto protocol of IASP basic pain terminology. Pain 2008; 137: 473–477.

Magerl W, Fuchs PN, Meyer RA, Treede RD. Roles of capsaicin-insensitive nociceptors in cutaneous pain and secondary hyperalgesia. Brain 2001; 124: 1754–1764.

Maier C, Baron R, Tölle TR, Binder A, Birbaumer N, Birklein F, Gierthmühlen J, Flor H, Geber C, Huge V, Krumova EK, Landwehrmeyer GB, Magerl W, Maihöfner C, Richter H, Rolke R,

Scherens A, Schwarz A, Sommer C, Tronnier V, Uçeyler N, Valet M, Wasner G, Treede RD. Quantitative sensory testing in the German Research Network on Neuropathic Pain (DFNS): somatosensory abnormalities in 1236 patients with different neuropathic pain syndromes. Pain 2010; 150 (3): 439-50.

Maris E and Oostenveld R. Nonparametric statistical testing of EEG- and MEG-data. J Neurosci Meth 2007; 164: 177–190.

Mouraux A and Iannetti GD. Across-trial averaging of event-related EEG responses and beyond. Magn Reson Imaging 2008; 26 (7): 1041-54.

Mouraux A, Guérit JM, Plaghki L. Non-phase locked electroencephalogram (EEG) responses to CO2 laser skin stimulations may reflect central interactions between Aδ- and C-fibre afferent volleys. Clin Neurophysiol 2003; 114 (4): 710-22.

Muthukumaraswamy SD. High-frequency brain activity and muscle artifacts in MEG/EEG: a review and recommendations. Front Hum Neurosci 2013; 7:138.

Nicholls ME, Thomas NA, Loetscher T and Grimshaw GM. The Flinders Handedness survey (FLANDERS): a brief measure of skilled hand preference. Cortex 2013; 49: 2914–2926.

Ploner M, Gross J, Timmermann L, Pollok B, Schnitzler A. Pain Suppresses Spontaneous Brain Rhythms. Cereb Cortex 2005; 16 (4): 537-540.

Sandkühler J. Understanding LTP in pain pathways. Mol Pain 2007; 3: 9.

Sandkühler J and Gruber-Schoffnegger D. Hyperalgesia by synaptic long-term potentiation (LTP): an update. Curr Opin Pharmacol 2012; 12 (1): 18–27.

Simone DA, Sorkin LS, Oh U, Chung JM, Owens C, LaMotte RH, Willis WD. Neurogenic hyperalgesia: central neural correlates in responses to spinothalamic tract neurons. J Neurophysiol 1991; 66: 228–246.

Tu Y, Zhang Z, Tan A, Peng W, Hung YS, Moayedi M, Iannetti GD, Hu L. Alpha and gamma oscillation amplitudes synergistically predict the perception of forthcoming nociceptive stimuli. Hum Brain Mapp 2016; 37 (2): 501-14.

Van den Broeke EN and Mouraux A. High frequency electrical stimulation of the human skin induces heterotopical mechanical hyperalgesia, heat hyperalgesia and enhanced responses to non-nociceptive vibrotactile input. J Neurophysiol 2014a; 111: 1564–1573.

Van den Broeke EN and Mouraux A. Enhanced brain responses to C-fiber input in the area of secondary hyperalgesia induced by high frequency electrical stimulation of the skin. J Neurophysiol 2014b; 112: 2059–2066.

Van den Broeke EN, Mouraux A, Groneberg AH, Pfau DB, Treede RD and Klein T. Characterizing pinprick evoked brain potentials before and after experimentally induced secondary hyperalgesia. J Neurophysiol 2015; 114: 2672–2681.

Van den Broeke EN, Lambert J, Huang G and Mouraux A. Central sensitization of mechanical nociceptive pathways is associated with a long-lasting increase of pinprick-evoked brain potentials. Front Hum Neurosci 2016a; 10: 531.

Van den Broeke EN, Lenoir C, Mouraux A. Secondary hyperalgesia is mediated by heat-insensitive A-fibre nociceptors. J Physiol 2016b; 594: 6767-6776.

Zhang ZG, Hu L, Hung YS, Mouraux A and Iannetti GD. Gamma-Band oscillations in the primary somatosensory cortex—A direct and obligatory correlate of subjective pain intensity. J Neurosci 2012; 32 (22): 7429-7438.

Ziegler EA, Magerl W, Meyer RA, Treede RD. Secondary hyperalgesia to punctate mechanical stimuli: central sensitization to A-fibre nociceptor input. Brain 1999; 122: 2245–2257.

FIGURE LEGENDS

Figure 1. Experimental set-up. **(A)** High frequency electrical stimulation of the skin (HFS) was applied to left or right volar forearm. Two different intensities of pinprick stimulation (64 and 96 mN) were applied to the skin surrounding the area onto which HFS was applied as well as to the same skin area on the contralateral arm, which served as control. **(B)** Characteristics of the HFS electrode. **(C)** The effect of HFS on the perception and brain responses elicited by the pinprick stimuli was assessed at two different time-points: before HFS and 20 minutes after applying HFS.

Figure 2. Effect of HFS on intensity and quality of perception elicited by the two pinprick intensities (64 and 96 mN). **(A)** Group-level average and standard deviation of the intensity of perception before and twenty minutes after applying HFS (numerical rating scale, NRS). Asterisks denote a statistically significant increase of the NRS scores after HFS at the HFS arm. **(B)** Group-level average proportion of trials reported as 'pinprick', 'touch' or 'undetected'. Almost all pinprick stimuli were perceived as 'pinprick' after HFS at the HFS arm.

Figure 3. (A) Group-level pinprick-evoked brain potentials recorded at Cz and elicited by the 64 mN stimulation intensity before and after applying HFS. **(B)** Group-level average difference waveforms (post minus pre HFS). The grey box shows the time-window during which the two waveforms were significantly different. **(C)** Individual amplitude of PEPs averaged within the time window in which the difference waveforms were significantly different. **(D)** Temporal evolution of the scalp topography within the time window in which the difference waveforms were significantly different. Shown is the difference in subtracted

waveforms (HFS_{post}-HFS_{pre} minus $control_{post}$-$control_{pre}$). Red and blue colours indicate an increase and decrease in PEP amplitude, respectively. Scalp topographies were flipped for the participants that received HFS to their left arm.

Figure 4. (A) Group-level pinprick-evoked potentials recorded at Cz and elicited by the 96 mN stimulation intensity before and after applying HFS. **(B)** Group-level difference waveforms (post minus pre HFS). No significant difference between the two difference waveforms was observed.

Figure 5. Group-level average time-frequency maps of low-frequency EEG activities (1-30 Hz) identified at electrode Cz including all time points (pre and post HFS) and sites (control and HFS arm), for the 64 mN stimulation intensity. **(A)** The TF-SINGLE maps are generated by averaging across trials the time-frequency maps of EEG amplitude obtained by applying the STFFT at single-trial level, thus revealing both phase-locked and non-phase-locked changes in EEG amplitude. **(B)** The TF-AVERAGE maps are generated by applying the STFFT to the time-domain average waveform, thus revealing only changes in the EEG signals that are phase-locked across trials. **(C)** Group-level average time-frequency maps of phase-locking value (PLV). Greater PLV values indicate time-frequency points at which the EEG signal is phase-locked across trials.

Figure 6. (A) Group-level average time-frequency maps of low-frequency EEG activities (1-30 Hz) obtained in the TF SINGLE transform at electrode Cz for the 64 mN stimulation intensity, pre and post HFS, at the control and HFS arm. **(B)** Time-frequency distribution of the cluster showing a significant increase of low-frequency activities**. (C)** Individual amplitude values of

the low frequency EEG activity within the cluster, pre and post HFS, at the control and HFS arm.

Figure 7. (A) Group-level average time-frequency maps of low-frequency EEG activities (1-30 Hz) obtained in the TF SINGLE transform at electrode Cz for the 96 mN stimulation intensity, pre and post HFS, at the control and HFS arm. **(B)** Time-frequency distribution of the cluster showing a significant increase in low-frequency activities. **(C)** Individual amplitude values of the low frequency EEG activity within the cluster, pre and post HFS, at the control and HFS arm.

Figure 8. Group-level average time-frequency maps of high-frequency EEG activities (30-100 Hz) obtained in the TF SINGLE transform at electrode Cz for the 64 mN stimulation intensity, pre and post HFS, at the control and HFS arm. No significant increase in high-frequency EEG activity respective to baseline and control arm was observed.

Figure 9. (A) Group-level average time-frequency maps of high-frequency EEG activities (30-100 Hz) obtained in the TF SINGLE transform at electrode Cz for the 96 mN stimulation intensity, pre and post HFS, at the control and HFS arm. **(B)** Time-frequency distribution of the cluster showing a significant increase in high-frequency activities.

SUPPLEMENTARY MATERIAL (Figures S1-3, video 1)

Supplementary Figure S1. Force profiles obtained during pinprick stimulation (64 mN) before and after training using force feedback. Shown are the normal forces **(A)** and tangential forces **(B)**. Black waveforms represent the average of 30 trials. Grey waveforms represent the standard deviation.

Supplementary Figure S2. Group-level average pinprick-evoked brain potentials (electrode Pz), merged for left and right arms and elicited by stimulation of non-sensitized skin in previous studies (Van den Broeke et al. 2015; Van den Broeke et al. 2016a) and in the present study. The figure shows the improved signal-to-noise ratio of PEPs obtained in the present study as compared to previous studies. This difference is attributed to the improved reproducibility of mechanical pinprick stimulation.

Supplementary Figure S3. Group-level average time-frequency maps of the EOG signal (30-100 Hz) obtained using the TF SINGLE transform, pre and post HFS, at the control and HFS arm, for electrode Cz **(A)** and electrode Pz **(C)**. Panels **B** and **D** shows the significant increase in high-frequency activity respective to baseline and control arm for the 64 mN (B) and 96 mN (D).

Video 1. Demonstration of pinprick stimulation.

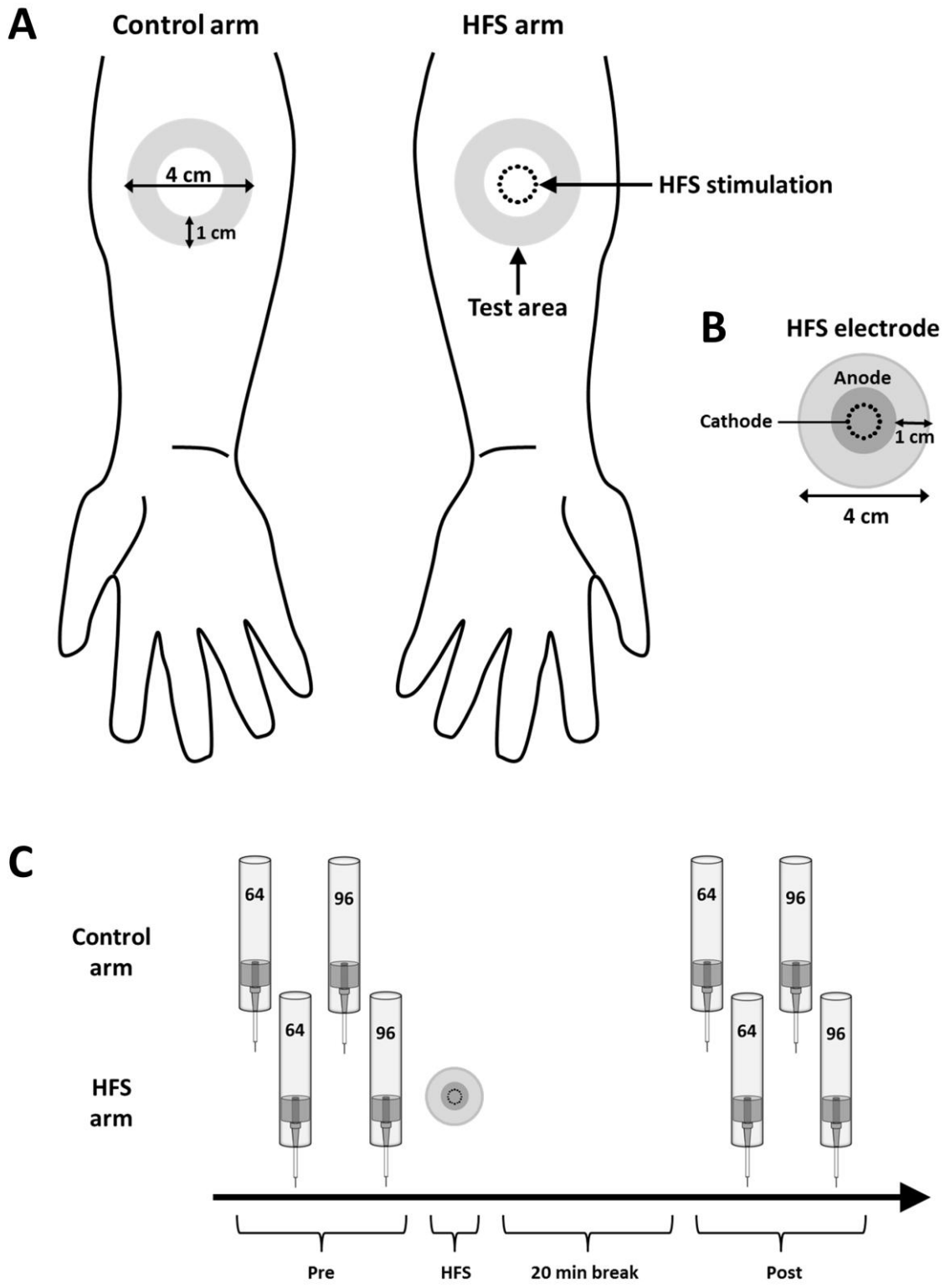
A
Control arm
HFS arm
4 cm
1 cm
HFS stimulation
Test area
B
HFS electrode
Anode
Cathode
1 cm
4 cm
C
Control arm
HFS arm
64
96
64
96
64
96
64
96
Pre
HFS
20 min break
Post

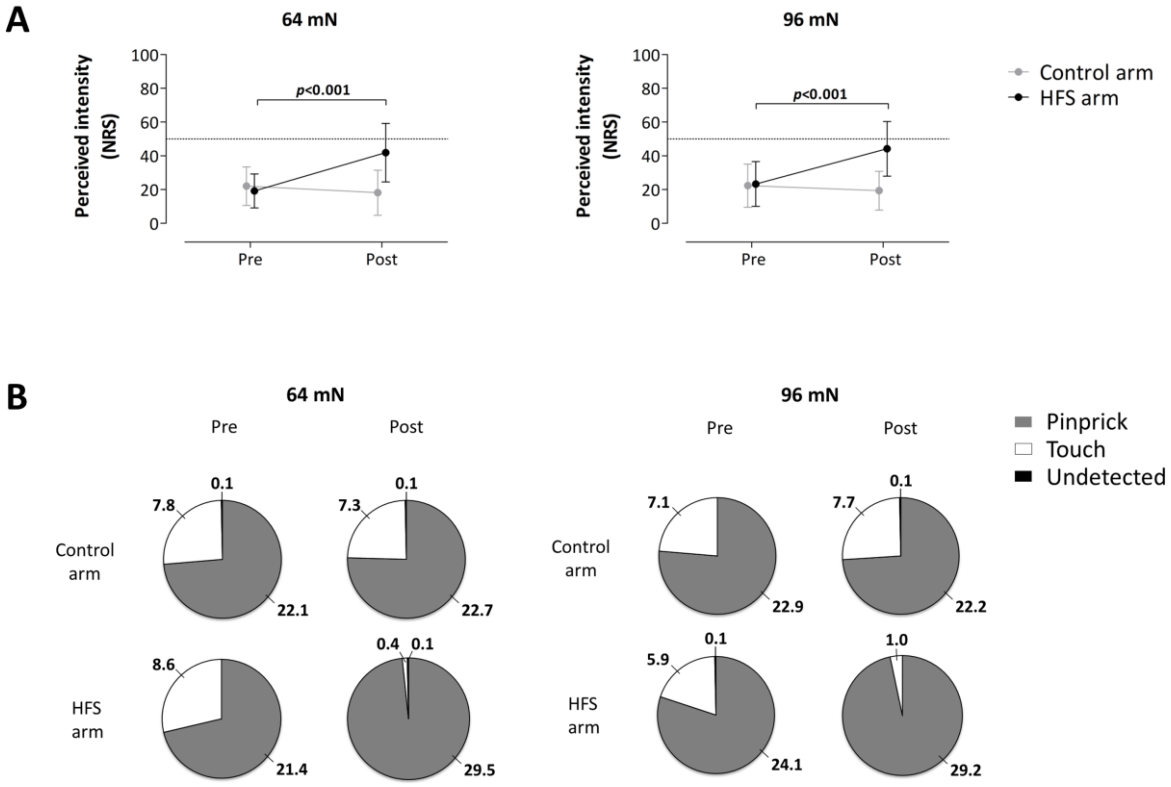

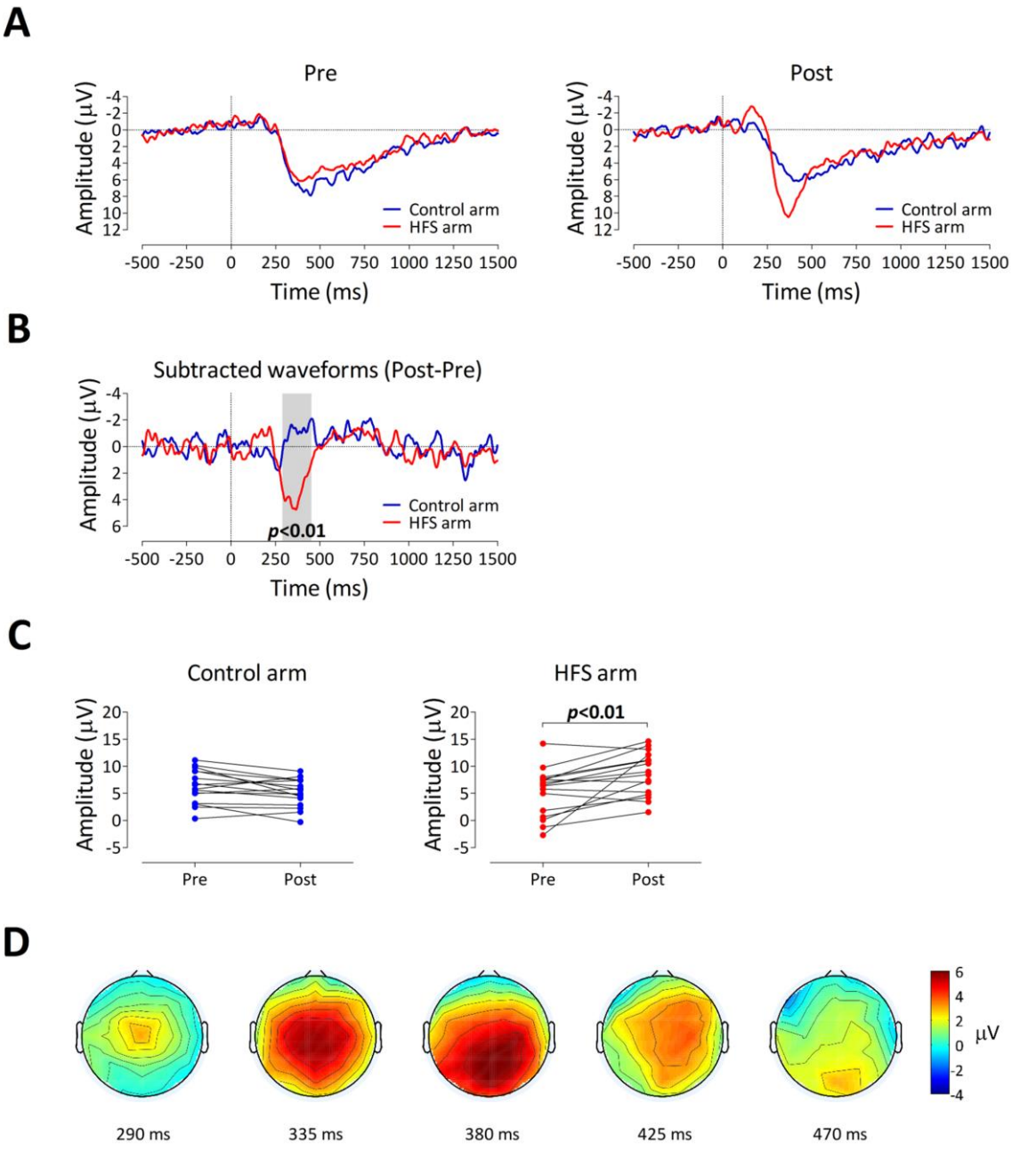
A
Pre
Post
Amplitude (μV)
Time (ms)
Control arm
HFS arm
B
Subtracted waveforms (Post-Pre)
p<0.01
C
Control arm
HFS arm
Pre
Post
D
290 ms
335 ms
380 ms
425 ms
470 ms
μV

A

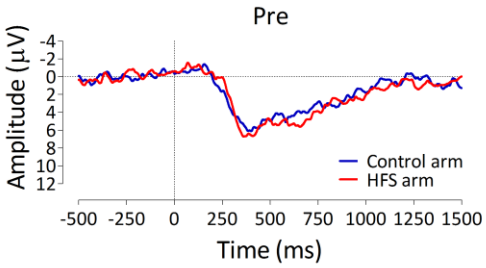

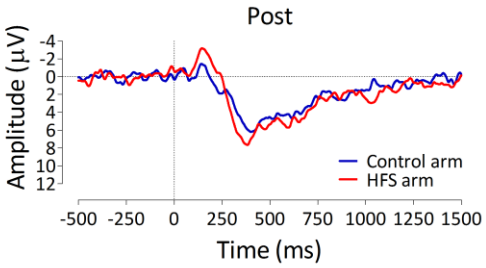

B